

A Molecular Model To Explain and Predict the Stereoselectivity in Rhodium-Catalyzed Hydroformylation†

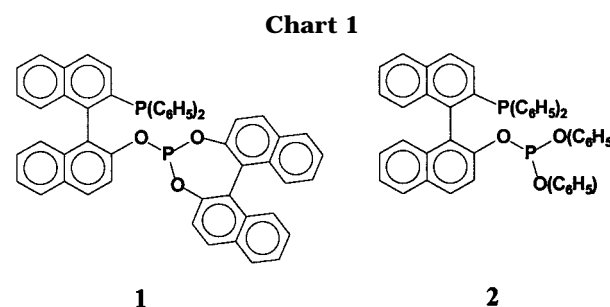
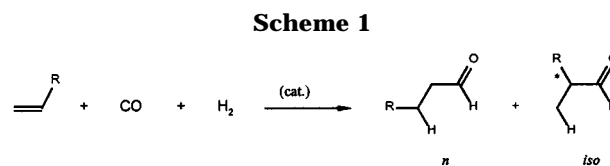
Dieter Gleich,[‡] Rochus Schmid,[§] and Wolfgang A. Herrmann*[‡]

Anorganisch-chemisches Institut, Technische Universität München,
Lichtenbergstrasse 4, D-85747 Garching, Germany, and Department of Chemistry,
University of Calgary, 2500 University Drive, Northwest, Calgary, Alberta, Canada T2N 1N4

Received February 25, 1998

Summary: By example of the bidentate phosphine–phosphite ligand BINAPHOS **1**, [(2-diphenylphosphino)-1,1'-binaphthalen-2-yl](1,1'-binaphthalen-2,2'-diyl)phosphite], a semiquantitative theoretical model elucidates the origin of stereodifferentiation in rhodium-catalyzed hydroformylation. It is demonstrated that the outstanding properties of **1** are due to the synergistic combination of three factors: (i) pronounced coordination preferences for steric and electronic reasons; (ii) adequate number of chirality centers; (iii) correct configuration of the binaphthyl fragments. The model is, in principle, applicable to all kinds of bidentate phosphine ligands.

Since the time hydroformylation was discovered by O. Roelen in 1938,¹ this reaction has become the largest-scale process of homogeneous organometallic catalysis.² On top of bulk chemical production (e.g., butyric aldehyde), hydroformylation would gain particular attraction if stereoselective catalysts were available³ because important chiral pharmaceuticals such as ibuprofen, naproxen, and others⁴ would then be conveniently accessible (*iso*-selectivity in Scheme 1). However, only a few examples of promising catalysts are documented in the literature: certain bimetallic platinum–tin systems effect hydrogenation as well as hydroformylation, while most rhodium catalysts give only low enantiomeric excesses (ee's).³ A breakthrough was landmarked by Takaya's discovery of the bidentate phosphine–phosphite ligand BINAPHOS (ligand **1** in Chart 1), which, in the presence of rhodium(I), gave asymmetric inductions of 82% ee for 2-butene and 94% ee for styrene without significant side reactions.⁵ Catalytic investigations with various substrates prove that the (*R,S*)- and (*S,R*)-enantiomers of the 2-fold axial chiral ligand yield high ee's, while the (*R,R*)- and (*S,S*)-isomers are significantly less selective.⁵ No molecular explanation of



this phenomenon has been available up to now, precluding any profound understanding of the hitherto unique ligand as well as strategies for further improvement. The model of Pino and Consiglio⁶ used by Takaya et al. to interpret their results^{5b} is purely qualitative and allows the extrapolation for other substrates on the basis of experimentally known selectivities only. However, prediction rather than reproduction should be the goal of any theoretical approach, but this is not a routine task. Quantum mechanical treatment of hydroformylation with ligand-modified rhodium catalysts⁷ has to rely on simplified model systems because otherwise the calculations become exceedingly time-consuming. Molecular mechanics (MM) calculations with more realistic systems, on the other hand, are much faster but cannot describe the course of chemical reactions, i.e., bond-forming and bond-breaking processes.⁸ Therefore, previous molecular mechanics work on asymmetric hydroformylation with platinum catalysts⁹ has been restricted to intermediates of the catalytic cycle. Suitable combinations of quantum and molecular mechanics can overcome both deficiencies.¹⁰

* To whom correspondence should be addressed. E-mail: lit@arthur.anorg.chemie.tu-muenchen.de.

† Dedicated to Professor Heinrich Nöth on the occasion of his 70th birthday.

‡ Technische Universität München.

§ University of Calgary.

(1) Reviews: (a) Herrmann, W. A.; Cornils, B. *Angew. Chem., Int. Ed. Engl.* **1997**, *36*, 1047. (b) Cornils, B.; Herrmann, W. A. In *Applied Homogeneous Catalysis with Organometallic Compounds*; VCH-Wiley: Weinheim, 1996; Vol. 1, pp 3–25. (c) Cornils, B.; Herrmann, W. A.; Rasch, M. *Angew. Chem., Int. Ed. Engl.* **1994**, *33*, 2144.

(2) (a) Frohning, C. D.; Kohlpaintner, C. W. In *Applied Homogeneous Catalysis with Organometallic Compounds*; VCH-Wiley: Weinheim, 1996; Vol. 1, pp 29–104. (b) Herrmann, W. A.; Kohlpaintner, C. W. *Angew. Chem., Int. Ed. Engl.* **1993**, *32*, 1524.

(3) Reviews: (a) Agbossou, F.; Carpentier, J.-F.; Mortreux, A. *Chem. Rev.* **1995**, *95*, 5. (b) Gladiali, S.; Bayon, J. C.; Claver, C. *Tetrahedron: Asymmetry* **1995**, *6*, 1453.

(4) Botteghi, C.; Paganelli, S.; Schionato, A.; Marchetti, M. *Chirality* **1991**, *3*, 355.

(5) (a) Horiuchi, T.; Shirakawa, E.; Nozaki, K.; Takaya, H. *Organometallics* **1997**, *16*, 2981. (b) Nozaki, K.; Sakai, N.; Nanno, T.; Higashijima, T.; Mano, S.; Horiuchi, T.; Takaya, H. *J. Am. Chem. Soc.* **1997**, *119*, 4413. (c) Sakai, N.; Nozaki, K.; Takaya, H. *J. Chem. Soc., Chem. Commun.* **1994**, 395. (d) Sakai, N.; Mano, S.; Nozaki, K.; Takaya, H. *J. Am. Chem. Soc.* **1993**, *115*, 7033.

(6) Consiglio, G.; Pino, P. *Top. Curr. Chem.* **1982**, *105*, 77.

(7) (a) Matsubara, T.; Koga, N.; Ding, Y.; Musaev, D. G.; Morokuma, K. *Organometallics* **1997**, *16*, 1065. (b) Koga, N.; Morokuma, K. *Chem. Rev.* **1991**, *91*, 823. (c) Koga, N.; Jin, S. Q.; Morokuma, K. *J. Am. Chem. Soc.* **1988**, *110*, 3417.

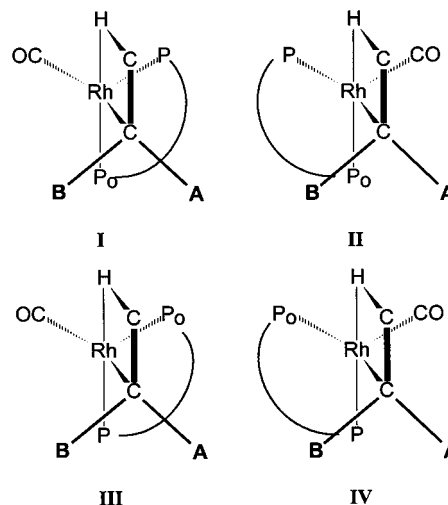
(8) Burkert, U.; Allinger, N. L. *Molecular Mechanics*; ACS Monograph 177; American Chemical Society: Washington, DC, 1982.

(9) Castonguay, L. A.; Rappé, A. K.; Casewit, C. J. *J. Am. Chem. Soc.* **1991**, *113*, 7177.

We have shown that the structure of chelating phosphines in metal complexes can be well-described by an accurately parametrized classical force field if the coordination geometry around the central metal is known.¹¹ Our semiquantitative theoretical approach is based on two assumptions supported by experiment:^{1,5a,12} (i) both the regio- and stereoselectivity of hydroformylation is exclusively determined during olefin insertion; (ii) the step of olefin insertion is irreversible. Only the relative energies of the transition states of olefin insertion must be determined to calculate the regio- and stereoselectivity of hydroformylation in this case.^{6,12,13a,14} In our model, an isolated molecule in the gas phase is considered, i.e., solvent effects are neglected. This simplification can be justified by the early nature of the transition states.^{13,14} To accurately describe the transition-state geometries in terms of their structures and energies, we performed density functional theory (DFT) calculations to model rhodium complexes bearing PH₃ ligands.^{13b,14,15–17} The transition states calculated for ethene and propene insertion into the Rh–H bond closely resemble the trigonal-bipyramidal starting geometry.^{13b,14} On the basis of these model-system transition states, force field calculations with the extended cff91 force field^{11,13,14,18,19} were carried out in order to incorporate steric effects. The geometry of the reaction center, e.g., the four-membered cycle of olefin insertion, was then taken from DFT calculations, as well as the approximately trigonal-bipyramidal coordination of the metal center. A complete force field parametrization was made without any external constraints.¹⁹ The global energetic minima have been searched for by molecular dynamics (MD) simulations.²⁰ All things considered, our strategy is distinct from related approaches.^{12,21}

NMR and IR investigations lead to the conclusion that the 1-coordinated olefin complexes are trigonal bipyramidal, with the ligand in an axial/equatorial arrangement and the phosphite–phosphorus atom (P_o in Scheme 2) in a trans position to the hydrido ligand.^{5b} These

Scheme 2. Coordination Modes I–IV of 1 in Trigonal–Bipyramidal Olefin Complexes^a



^a A and B label substituent positions as well as *iso*-transition states.

restrictions arise from the electronic and steric situation²² and permit only the two coordination modes I and II but not III and IV (Scheme 2). We first consider the insertion of a *terminal* olefin. Four transition states are generally possible: two leading to linear *n*-aldehydes and the other two yielding branched *iso*-aldehydes distinguished by one stereocenter (Scheme 2). Conjugated olefins such as styrene show different regioselectivities than aliphatic olefins.³ We discard the treatment of regioselectivities here since styrene is experimentally known to form mainly *iso*-aldehydes.³ It is, thus, more interesting to focus on the energetic differentiation between the diastereomeric transition states A and B (Scheme 2). The relative energies of the global minima²⁰ calculated for the styrene insertion are listed in Table 1. The high ee's achieved with 1-(*R,S*) originate from the unexpected fact that both coordination modes I and II favor transition state A leading to the (*R*)-aldehyde, the enantiomer which is also observed experimentally.^{5b,c} The four calculated transition-state structures of 1-(*R,S*) are depicted in Figure 1. Transition state A is lower in energy than its alternative B

(20) Suitable initial structures were subject to two independent MD simulations: (1) The temperature (1000 K) was held constant for 100 ps. Every picosecond the structure was minimized. (2) There were 2.4 ps cycles with falling temperature (1000–300 K) and two minimizations repeated 50 times. The first minimization was done after a 0.5 ps sampling at 1000 K, the second after a 0.5 ps sampling at 300 K. Between these two samplings, the temperature was lowered by 50 K steps every 0.1 ps. The lowest energy structures of both simulations (which have proven to be identical) were taken as global minima. The calculations of ee's follow the formula (2 *iso* transition states *a* and *b*, *T* = 298 K)

$$ee (\%) = \frac{e - \left(\frac{E_{iso,a}^{\ddagger} - E_{iso,b}^{\ddagger}}{R \cdot T} \right) - 1}{e - \left(\frac{E_{iso,a}^{\ddagger} - E_{iso,b}^{\ddagger}}{R \cdot T} \right) + 1} \times 100$$

In this formula, changes of temperature have only a small influence. All MM calculations were performed with the Insight/Discover program package (Insight/Discover, Release 95.0, BIOSYM/MSI: San Diego, 1995).

(21) Nozaki, K.; Sato, N.; Tonomura, Y.; Yasutomi, M.; Takaya, H.; Hiwama, T.; Matsubara, T.; Koga, N. *J. Am. Chem. Soc.* **1997**, *119*, 12779.

(22) (a) MM calculations suggest a rather rigid ligand structure with a natural bite angle near 90° (cf. refs 5c, 13a, 14, and 22b). (b) Casey, C. P.; Whiteker, G. T. *Isr. J. Chem.* **1990**, *30*, 299.

(10) (a) Maseras, F.; Morokuma, K. *J. Comput. Chem.* **1995**, *16*, 1170. (b) Kuribayashi, H. K.; Koga, N.; Morokuma, K. *J. Am. Chem. Soc.* **1992**, *114*, 8687.

(11) (a) Herrmann, W. A.; Schmid, R.; Kohlpaintner, C. W.; Priemeier, T. *Organometallics* **1995**, *14*, 1961. (b) Schmid, R. Diploma Thesis, Technische Universität München, Germany, 1993.

(12) Casey, C. P.; Petrovich, L. M. *J. Am. Chem. Soc.* **1995**, *117*, 6007.

(13) (a) Gleich, D. Diploma Thesis, Technische Universität München, Germany, 1997. (b) Schmid, R. Ph.D. Thesis, Technische Universität München, Germany, 1997.

(14) Herrmann, W. A.; Schmid, R.; Gleich, D. Manuscript in preparation.

(15) The calculations on the BP86/DZVP//LDA/DZVP level (cf. refs 16 and 17a) are related to Morokuma's ab initio (HF and MP2) results (cf. ref 7) but aim at complexes with *two* phosphorus ligands. All DFT calculations were performed with the program DGauss (DGauss, Release 3.0, Cray Research Inc., 1995; cf. ref 17b).

(16) (a) Becke, A. *Phys. Rev. A* **1988**, *38*, 3098. (b) Perdew, J. P. *Phys. Rev. B* **1986**, *33*, 8822.

(17) (a) Godbout, N.; Salahub, D. R.; Andzelm, J.; Wimmer, E. *Can. J. Chem.* **1992**, *70*, 560. (b) Andzelm, J.; Wimmer, E. *J. Chem. Phys.* **1992**, *96*, 1280.

(18) Maple, J. R.; Dinur, U.; Hagler, A. T. *Proc. Natl. Acad. Sci. U.S.A.* **1988**, *85*, 5350.

(19) Force field parameters were derived as far as possible to reproduce the DFT structure of the reaction center. The approximately trigonal-bipyramidal metal coordination was regulated by soft restraints implemented in the force field. Atomic charges other than those of aryl rings were neglected. A detailed description of the parametrization process can be found in refs 13a and 14. Parameters for phosphorus are listed in ref 11a; further parameters are given as Supporting Information.

Table 1. Transition States (TS) for Styrene

ligand	coordination mode ^a	TS ^a	E [‡] (kcal mol ⁻¹) ^b	ee (%) ^c (config)	ee (%) ^d (config)
1-(R,S)	I	A	0	90 (<i>R</i>)	~90 (<i>R</i>)
		B	1.8		
	II	A	0	>99 (<i>R</i>)	
		B	7.1		
	I	A	5.6	>99 (<i>S</i>)	~25 (<i>R</i>)
		B	0		
	II	A	0	98 (<i>R</i>)	
		B	2.7		
	I	A	3.4	>99 (<i>S</i>)	
		B	0		
	II	A	0	>99 (<i>R</i>)	
		B	4.8		
	III	A	6.6	>99 (<i>S</i>)	
		B	0		
IV	A	0	79 (<i>R</i>)		
	B	1.3			

^a Cf. Scheme 2. ^b Relative energy of transition state. ^c Calculated (cf. ref 20). ^d Observed (cf. ref 5b).

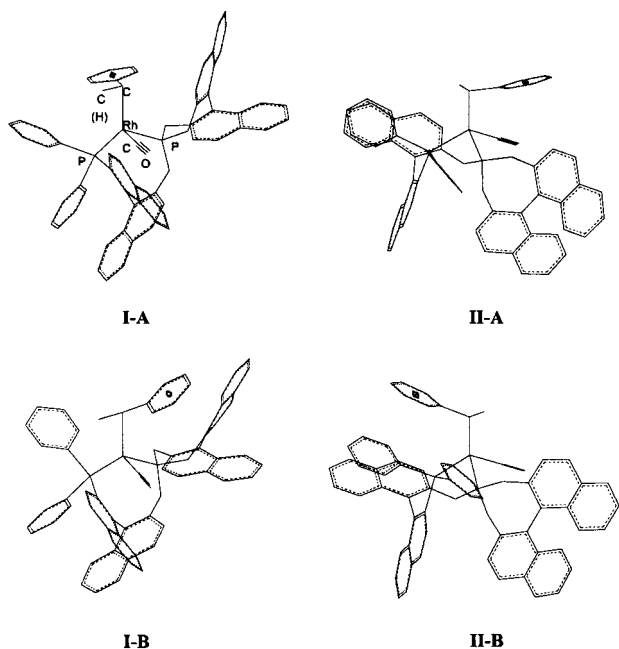


Figure 1. Calculated transition-state structures for **1-(R,S)**. The phenyl group of styrene is marked with an asterisk; hydrogens are omitted for clarity.

for *both* coordination modes **I** and **II**. This clearly rules out the picture of only *one* preferred coordination mode as assumed by Pino's model.^{5b,6} In contrast, in the case of (*R,R*)-BINAPHOS **1-(R,R)**, coordination modes **I** and **II** favor transition states **A** and **B**, respectively. Hence, the net asymmetric induction achieved with **1-(R,R)** is low. This result is in accord with experimental observation too^{5b,c} but definitely cannot be explained by Pino's model. Our model is also applicable to *internal* olefins, exemplified by 2-butene occurring as the two isomers (*E*) and (*Z*). Again, two diastereomeric transition states **A** and **B** are possible for (*E*) and (*Z*), respectively (Scheme 2). Tables 2 and 3 summarize the energies calculated for the insertion of 2-butene and show that systems employing **1-(R,S)** prefer transition state **A** exclusively and yield the experimentally observed (*S*)-aldehyde^{5b,c} with high stereodifferentiation. On the other hand, systems employing **1-(R,R)** prefer transition states with opposite selectivities and achieve considerably lower asymmetric induction.

Table 2. Transition States (TS) for (*E*)-2-Butene

ligand	coordination mode ^a	TS ^a	E [‡] (kcal mol ⁻¹) ^b	ee (%) ^c (config)	ee (%) ^d (config)
1-(R,S)	I	A	0	99 (<i>S</i>)	48 (<i>S</i>)
		B	3.5		
	II	A	0	88 (<i>S</i>)	
		B	1.6		
	I	A	0.2	21 (<i>R</i>)	low
		B	0		
II	A	0	40 (<i>S</i>)		
	B	0.5			

^a Cf. Scheme 2. ^b Relative energy of transition state. ^c Calculated (cf. ref 20). ^d Observed (cf. ref 5b).

Table 3. Transition States (TS) for (*Z*)-2-Butene

ligand	coordination mode ^a	TS ^a	E [‡] (kcal mol ⁻¹) ^b	ee (%) ^c (config)	ee (%) ^d (config)
1-(R,S)	I	A	0	95 (<i>S</i>)	82 (<i>S</i>)
		B	2.2		
	II	A	0	>99 (<i>S</i>)	
		B	3.6		
	I	A	2.1	93 (<i>R</i>)	low
		B	0		
II	A	0	96 (<i>S</i>)		
	B	2.6			

^a Cf. Scheme 2. ^b Relative energy of transition state. ^c Calculated (cf. ref 20). ^d Observed (cf. ref 5b).

Our results lead to the general conclusion that **1-(R,S)** (or **1-(S,R)**) enforces asymmetric induction while **1-(R,R)** (or **1-(S,S)**) has a detrimental effect. In the first case, both coordination modes favor the same olefin orientation, whereas in the second case, opposite preferences cancel out each other. Synergism and antagonism of two chirality centers are reminiscent of the concept of "matched" and "mismatched" stereoselection.²³ If one chirality center (ligand **2-(R)**; Chart 1) is eliminated, the advantageous synergism is destroyed (Table 1): coordination modes **I** and **II** favor opposite transition states. Yet two chirality centers seem to be a necessary but not a sufficient condition for high asymmetric induction. This can be seen from calculations regarding coordination modes **III** and **IV** of **1-(R,S)** (Table 1, Scheme 2): the stereoselectivity is also lowered by antagonism. It is, therefore, the suitable combination of three factors that accounts for the outstanding properties of the Takaya ligand: (i) pronounced coordination preferences (**I** and **II**) for steric *and* electronic reasons; (ii) adequate number of chirality centers; (iii) correct configuration of the binaphthyl fragments (*R,S* or *S,R*).

Our model is able to give a convincing explanation for the origin of stereodifferentiation which is, in principle, applicable to all kinds of bidentate phosphine ligands. It merges theoretically as well as experimentally derived conclusions, thus combining the power of both strategies. We are presently designing new ligands comprised of the advantages of **1-(R,S)**.

Acknowledgment. This work was generously supported by the Deutsche Forschungsgemeinschaft and the Fonds der Chemischen Industrie.

Supporting Information Available: Tables of force field parameters, force field potentials, and coordinates of several structures (8 pages). Ordering information is given on any current masthead page.

OM9801397

(23) Masamune, S.; Choy, W.; Petersen, J. S.; Sita, L. R. *Angew. Chem., Int. Ed. Engl.* **1985**, *24*, 1.